

Lhx2 specifies regional fate in Emx1 lineage of telencephalic progenitors generating cerebral cortex

Shen-Ju Chou, Carlos G Perez-Garcia, Todd T Kroll & Dennis D M O'Leary

Cerebral cortex is comprised of regions, including six-layer neocortex and three-layer olfactory cortex, generated by telencephalic progenitors of an Emx1 lineage. The mechanism specifying region-specific subpopulations in this lineage is unknown. We found that the LIM homeodomain transcription factor *Lhx2* in mice, expressed in graded levels by progenitors, determines their regional identity and fate decisions to generate neocortex or olfactory cortex. Deletion of *Lhx2* with *Emx1-cre* at embryonic day 10.5 (E10.5) altered the fates of progenitors, causing them to generate three-layer cortex, phenocopying olfactory cortex rather than lateral neocortex. Progenitors did not generate ectopic olfactory cortex following *Lhx2* deletion at E11.5. Thus, *Lhx2* regulates a regional-fate decision by telencephalic progenitors during a critical period that ends as they differentiate from neuroepithelial cells to neuronogenic radial glia. These findings establish a genetic mechanism for determining regional-fate in the Emx1 lineage of telencephalic progenitors that generate cerebral cortex.

The mammalian cerebral cortex is comprised of several major regions, including six-layer neocortex and architecturally more simple and phylogenetically older cortices, such as three-layer paleocortex, which is predominantly olfactory cortex (that is, piriform cortex) and archicortex, which is predominantly hippocampal formation¹. The majority of neurons that form each region, including all glutamatergic and projection neurons, arise from a progenitor lineage in the ventricular zone of dorsal telencephalon (dTel) that is defined by the expression of *Emx1*, a homeodomain transcription factor². However, little progress has been made on defining the mechanisms that determine distinct regional fates in this relatively uniform population of progenitors.

Although expression of *Emx1* is a defining characteristic of dTel progenitors, the expression of *Emx1* or of any transcription factor has not been shown to determine the regional fate of progenitors in the Emx1 lineage. Furthermore, the Emx1 progenitor lineage has not been subdivided into distinct populations, or sublineages, that generate specific regions of cerebral cortex by their expression of a distinct transcription factor. Indeed, such a relationship between a lineage and a specific region of cerebral cortex might not exist. However, unique subpopulations of progenitors of the Emx1 lineage must generate distinct regions of cerebral cortex and must be specified by their unique expression of one or more transcription factors. The mechanism for specifying regional fate in the Emx1 lineage may involve a graded expression of a transcription factor that defines unique subpopulations of progenitors via differences in expression levels. The LIM homeodomain transcription factor *Lhx2*, which is expressed in all dTel progenitors of the Emx1 lineage in a high-to-low caudomedial-to-rostralateral graded pattern across the dTel ventricular zone^{3,4}, is a strong candidate for this role.

Lhx2 is a critical regulator of cortical development and may function as a selector gene for cortical identity. For example, analysis of

an *Lhx2* constitutive knockout shows that cerebral cortex largely fails to form because ventricular zone progenitors become quiescent early in corticogenesis, although some markers associated with piriform cortex are detectable⁵. Furthermore, a patterning center, the cortical hem, expands and overpopulates the cortical wall with Cajal-Retzius neurons^{3,4,6}. In addition, clusters of *Lhx2*^{-/-} neurons in dorsomedial neocortex of chimeric mice made from *Lhx2*^{-/-} and wild-type blastula do not express neocortical markers⁷.

We examined *Lhx2*'s role in the specification of regional fate in dTel progenitors of the Emx1 lineage, hypothesizing that *Lhx2* regulates the fate decision in this lineage to produce neocortex or paleocortical piriform cortex. Because of severe defects in *Lhx2* constitutive knockout mice and their embryonic lethality³, we generated a conditional knockout (cKO) of *Lhx2*. We generated mice with *loxP*-flanked alleles of *Lhx2* and used three different lines of mice that expressed Cre recombinase, *Emx1-cre*⁸, *Nestin-cre*⁹ and *Nex-cre*¹⁰, to delete *Lhx2* at different times to assess *Lhx2*'s involvement in the specification and fate of dTel progenitors and their progeny that form cerebral cortex. *Lhx2* expression begins in forebrain at E8.5 before neurulation, 2 d before the earliest Cre-mediated deletion of *loxP*-flanked alleles^{4,6} with *Emx1-cre*, allowing transient expression of *Lhx2* in dTel progenitors to promote development of cerebral cortex, which was crucial for our study.

We found that *Lhx2* regulated a fate decision among dTel progenitors of the Emx1 lineage to generate phylogenetically distinct telencephalic regions, lateral neocortex or paleocortical piriform cortex, and was required for progenitors of lateral neocortex and their progeny to acquire a neocortical fate. *Lhx2* regulated this fate decision in a critical period that ended with the differentiation of neuronogenic radial glia and onset of cortical neurogenesis. These findings establish a genetic mechanism for determining the regional fate of dTel progenitors of the Emx1 lineage that generate cerebral cortex.

Molecular Neurobiology Laboratory, The Salk Institute, La Jolla, California, USA. Correspondence should be addressed to D.D.M.O (doleary@salk.edu).

Received 30 July; accepted 14 September; published online 11 October 2009; doi:10.1038/nn.2427

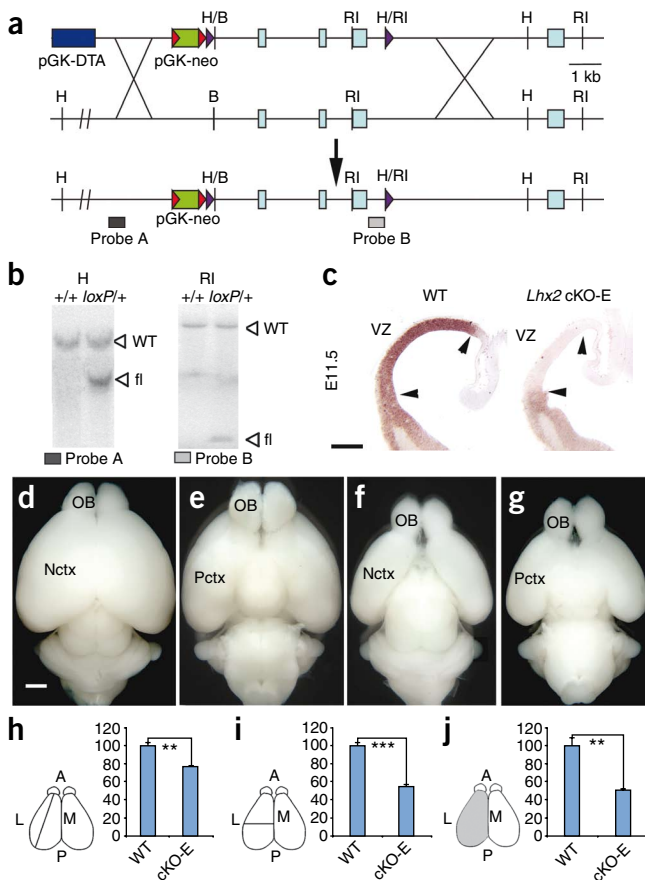


Figure 1 Generation of the *loxP*-flanked allele of *Lhx2* and conditional deletion using *Emx1-cre*. **(a)** Targeting strategy. Red and purple triangles indicate *FRT* and *loxP* sites. B, BamHI; H, HindIII; RI, EcoRI restriction enzyme sites. **(b)** Southern hybridization of wild-type (WT, +/+) and heterozygous (*loxP*/+) embryonic stem cell clones with probes A and B. Genomic DNA was digested with *Hind*III (H) and hybridized with probe A, and we found a 10-kb wild-type band and a 6-kb floxed band (fl). Probe B and *Eco*RI (RI) digestion revealed a 15-kb wild-type band and a 2-kb floxed band. **(c)** *In situ* hybridization for *Lhx2* on E11.5 wild-type and cKO-E coronal sections showed selective deletion in dorsal telencephalon (arrowheads) in cKO-E ventricular zone (VZ). Scale bar represents 0.2 mm. **(d–g)** Dorsal (**d,f**) and ventral (**e,g**) views of P7 wild-type (**d,e**) and cKO-E (**f,g**) brains. cKO-E neocortex (Nctx) was reduced in size. **(h)** Relative neocortical anterior-posterior length in wild-type and cKO-E mice. The wild-type length mean is set as 100. Compared with wild type (100 ± 3.14 , $n = 4$), the length of cKO-E neocortex (76.54 ± 1.20 , $n = 4$) was significantly decreased ($P < 0.01$, unpaired Student's *t* test). **(i)** Relative neocortical width (from midline to lateral side). The wild-type width mean is set as 100. Compared with wild type (100 ± 3.44 , $n = 4$), the neocortical width of cKO-E (54.83 ± 1.98 , $n = 4$) was significantly decreased ($P < 0.001$). **(j)** Relative dorsal surface area of the cerebral hemisphere. The wild-type surface area mean is set as 100. Compared with wild type (100 ± 9.88 , $n = 4$), the cKO-E surface area (50.75 ± 1.06 , $n = 4$) was significantly decreased ($P < 0.01$). Scale bar represents 0.5 mm. A, anterior; L, lateral; M, medial; OB, olfactory bulb; P, posterior; Pctx, paleocortex. Error bars represent \pm s.e.m. ** indicates $P < 0.01$ and *** indicates $P < 0.001$.

RESULTS

Neocortical-paleocortical shifts following *Lhx2* deletion

Mice with *loxP*-flanked alleles of *Lhx2* were generated and initially crossed with an *Emx1-cre* line⁸ to delete *Lhx2* from progenitors of the *Emx1* lineage that give rise to cerebral cortex (**Fig. 1**). The *Lhx2*^{*loxP*/+}; *Emx1-cre* and *Lhx2*^{*loxP*/loxP}; *Emx1-cre* offspring were postnatal viable, exhibited the same phenotype and were grouped as cKO-E. We obtained an additional five genotypes as littermates from these crosses (*Lhx2*^{*loxP*/-} without *Emx1-cre*, *Lhx2*^{*loxP*/+} or *Lhx2*^{*loxP*/-}, with or without *Emx1-cre*), which had similar phenotypes and were grouped as wild types.

To examine regional patterning of telencephalon deficient for *Lhx2*, we carried out whole-mount *in situ* hybridization at postnatal day 0 (P0) with a neocortical marker, *Satb2* (ref. 11), and a paleocortical marker, *Nrp2* (ref. 12). In wild-type mice, *Satb2* marked the dorsal-dorsolateral surface of the cortical hemisphere and *Nrp2* marked, in a complementary fashion, the ventral-ventrolateral surface (**Fig. 2**). In cKO-E mice, the telencephalon was smaller and exhibited aberrant patterning. The *Satb2* domain was substantially reduced, with its ventrolateral border shifted dorsally, and was striped as a result

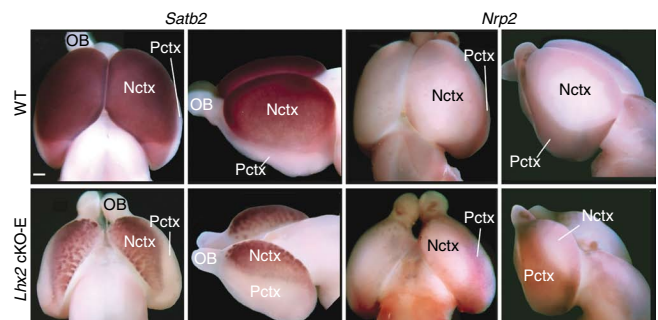
Figure 2 Complementary changes in neocortical and paleocortical domains in cerebral cortex of cKO-E mice following *Lhx2* deletion by *Emx1-cre*. Whole-mount *in situ* hybridization of P0 wild-type (*Lhx2*^{*loxP*/+}; *Emx1-cre*) and *Lhx2* cKO-E (*Lhx2*^{*loxP*/-}; *Emx1-cre*) brains using the neocortex marker *Satb2* and the paleocortex (Pctx) marker *Nrp2* shown from dorsal (rostral to the top) and side (rostral to the left) views. Compared with wild type, the *Satb2* expression domain was reduced in size in the *Lhx2* cKO-E and its ventral border shifted dorsally in the cortical hemisphere, complemented by an expansion and dorsal shift of the *Nrp2* expression domain. Scale bar represents 0.5 mm.

of diminished staining of cell-sparse domains that alternated with cell-dense domains in superficial layers (**Fig. 2**). The *Nrp2* domain exhibited a parallel change to the *Satb2* domain, shifting dorsally to retain its complementary expression pattern with *Satb2* (**Fig. 2**). Thus, deletion of *Lhx2* from progenitors of the *Emx1* lineage results in a substantial change in telencephalic patterning, with an expansion of paleocortical markers and a restriction of neocortical markers.

We carried out a marker analysis to assess the integrity and positioning of cortical hem, which is a caudomedial patterning center¹³, the pallium-subpallium boundary (PSB), and anti-hem, a putative ventrolateral patterning center coincident with PSB¹⁴, and found no differences between cKO-E and wild-type (**Supplementary Results and Supplementary Fig. 1**). Furthermore, expression of the transcription factors *Dlx2*, *Dlx5*, *Gsx2* (*Gsh2*), *Ascl1* (*Mash1*) and *Arx*, which have been implicated in specifying fates of neurons generated in the lateral ganglionic eminence^{15–18}, a prominent germinal zone of ventral telencephalon that is contiguous to the dTel ventricular zone, remained limited to the lateral ganglionic eminence (**Supplementary Fig. 2**). Thus, the effects of *Lhx2* on neocortical versus paleocortical fate are probably the result of it directly influencing dTel progenitors of the *Emx1* lineage.

ePC forms following *Lhx2* deletion from *Emx1* lineage

To determine the outcome of expansion of the paleocortical marker *Nrp2* that we observed at P0 on underlying telencephalic patterning,



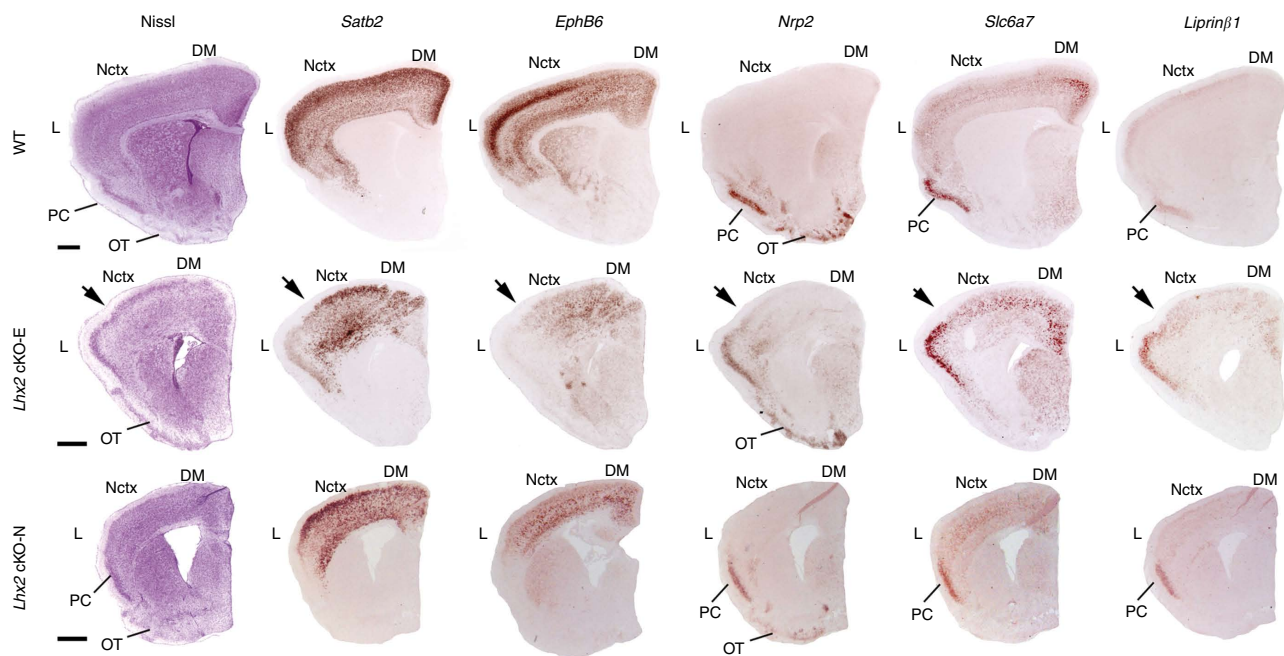


Figure 3 Altered patterns of regional telencephalic markers demonstrate a re-fating of lateral neocortex into piriform cortex following *Lhx2* deletion with *Emx1-cre*, but not *Nestin-cre*. Nissl staining and *in situ* hybridization for the neocortex markers *Satb2* and *EphB6*, the paleocortex marker *Nrp2* and the piriform cortex (PC) markers *Slc6a7* and *Liprinβ1* on coronal sections of P7 wild-type (*Lhx2^{loxP/+}*), *Lhx2* cKO-E (*Lhx2^{loxP/-}; Emx1-cre*) and *Lhx2* cKO-N (*Lhx2^{loxP/-}; Nestin-cre*) brains. In wild types, *Satb2* and *EphB6* were expressed in both dorsomedial (DM) and lateral (L) neocortex, whereas *Nrp2* was expressed in piriform cortex and olfactory tubercle (OT) and *Slc6a7* and *Liprinβ1* were expressed specifically in piriform cortex. In wild types, piriform cortex was located ventrally in the cortical hemisphere. In *Lhx2* cKO-E mice, high levels of *Satb2* and *EphB6* expression were detected in dorsomedial neocortex and not in lateral neocortex; instead, we found ectopic expression of *Nrp2*, *Slc6a7* and *Liprinβ1* in the lateral neocortex that was coincident with the ectopic three-layer piriform cortex seen in the Nissl staining. The transition between these two patterns in dorsomedial and lateral neocortex is marked with an arrow. In *Lhx2* cKO-N mice, *Nrp2*, *Slc6a7* and *Liprinβ1* labeled wild-type piriform cortex that was located ventrally, whereas lateral neocortex was strongly labeled by *Satb2* and *EphB6*, as in wild type. In *Lhx2* cKO-E mice, *Satb2* expression persisted throughout the ePC in place of lateral neocortex, although at substantially diminished levels relative to lateral neocortex in wild types and to dorsomedial neocortex in *Lhx2* cKO-E mice. *Satb2* expression was not detected in wild-type piriform cortex. Scale bar represents 0.5 mm.

we focused our analyses on P7, when laminar organization of cerebral cortex is mature. Nissl staining and *in situ* hybridization were carried out on sections from P7 wild-type and cKO-E littermates using *Nrp2* (ref. 12) and the neocortical markers *Satb2* and *EphB6* (refs. 11,19) (Fig. 3). Because *Nrp2* marks the contiguous olfactory cortical structures, piriform cortex and olfactory tubercle, we selected *Slc6a7* (ref. 20) and *Ppfbp1* (*Liprinβ1*)²¹ from the Allen Brain Atlas (<http://www.brain-map.org>) and the Brain Gene Expression Map (<http://www.stjudebgem.org>) and confirmed that each marked piriform cortex and distinguished it from olfactory tubercle and adjacent neocortex (Fig. 3).

Compared with wild type, the neocortex of cKO-E mice was reduced in size and had two distinct, aberrant lamination patterns. In dorsomedial neocortex of cKO-E mice, both of the neocortical markers, *Satb2* and *EphB6*, had a roughly wild type-like expression pattern and *Nrp2* was largely absent (Fig. 3). In contrast, in lateral neocortex, expression of *Satb2* and *EphB6* was diminished and was replaced by robust expression of *Nrp2*, and six-layer architecture characteristic of neocortex was replaced by a three-layer architecture resembling piriform cortex (Fig. 3). In addition, this ectopic *Nrp2* domain expressed the piriform cortex markers *Slc6a7* and *Liprinβ1*, which distinguished it from the *Nrp2*-positive olfactory tubercle (Fig. 3), indicating that this aberrant structure positioned in lateral neocortex is an ectopic piriform cortex (ePC). In contrast, the *Nrp2*-positive three-layer cortical structure ventral to ePC was not marked by either *Slc6a7* or *Liprinβ1*, indicating that it is olfactory tubercle (Fig. 3). Thus, following

conditional deletion of *Lhx2* using *Emx1-cre*, lateral neocortex was replaced by a cortical structure that had the architecture and marker expression of piriform cortex and a wild-type piriform cortex was not identified at its normal ventral position. These findings strongly suggest that progenitors that normally generate lateral neocortex are re-fated to generate piriform cortex following deletion of *Lhx2* using *Emx1-cre*.

We used immunostaining to assess the expression of the projection neuron marker *Bcl11b* (*Ctip2*) relative to *Satb2* at P7 (Fig. 4). In wild-type mice, *Ctip2* is preferentially expressed by layer 5 projection neurons in neocortex, whereas it strongly labels layer 2 in piriform cortex and olfactory tubercle²². In cKO-E mice, *Ctip2* was expressed in layer 2 of ePC, coincident with expression of the paleocortical marker *Nrp2* (Fig. 4), and retained a wild type-like expression pattern in dorsomedial neocortex, coincident with expression of the neocortical marker *Satb2* (Fig. 4). Although *Satb2* expression in ePC was considerably lower than in wild-type neocortex or in dorsomedial neocortex of cKO-E mice, its expression persisted throughout ePC and was nondetectable in wild-type piriform cortex (Figs. 3 and 4). *EphB6* expression was reduced to nondetectable levels in ePC. The maintained, albeit substantially reduced, expression of the neocortical marker *Satb2* in ePC after *Lhx2* deletion is strong evidence that it is indeed generated by progenitors of the *Emx1* lineage that would normally generate lateral neocortex, but are re-fated to generate piriform cortex.

To further determine the degree of re-fating, we analyzed the connectivity of ePC in P7 cKO-E mice and found that it receives afferent

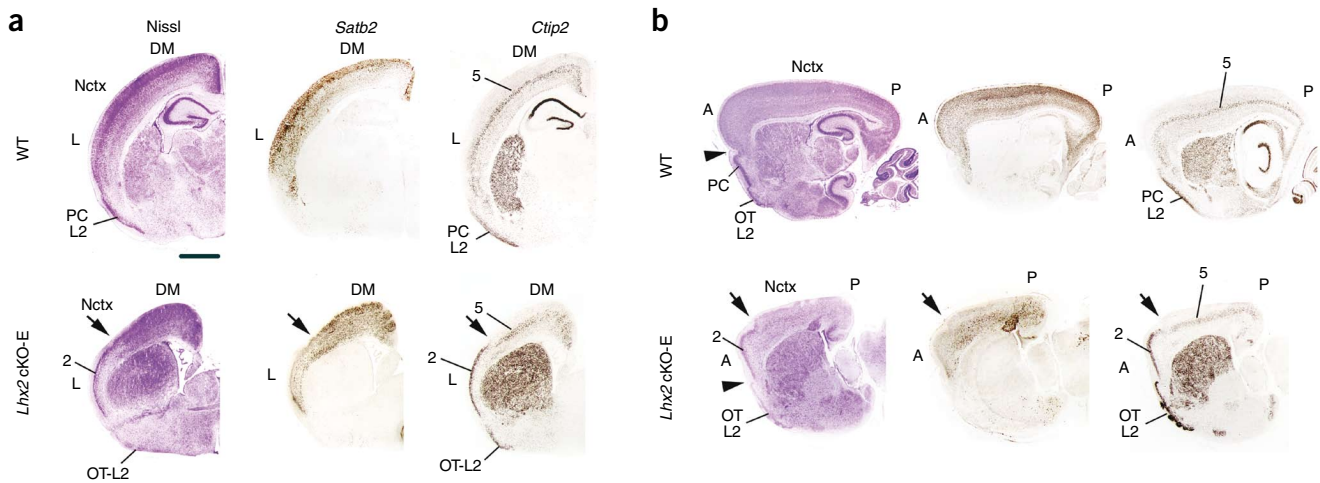


Figure 4 Distinct expression patterns of *Ctip2* and *Satb2* in *Lhx2* cKO-E telencephalon indicate that lateral neocortex is re-fated into piriform cortex. **(a,b)** Nissl and immunostaining of adjacent coronal **(a)** and sagittal **(b)** sections from P7 wild-type and *Lhx2* cKO-E brains with *Satb2*, a neocortex (Nctx) marker, and *Ctip2*, a neocortical layer 5 and paleocortical layer 2 marker. **(a)** In wild types, *Ctip2* was expressed in neocortical layer 5 (5) and in layer 2 of piriform cortex (PC-L2), and *Satb2* was robustly expressed in neocortex. *Satb2* expression was strongly diminished in lateral neocortex of *Lhx2* cKO-E compared with wild type, coincident with the change from six-layer neocortex to a three-layer architecture of ePC; *Ctip2* was expressed in layer 5 of dorsomedial neocortex, layer 2 of ectopic piriform cortex (2) and layer 2 of olfactory tubercle (OT-L2). The transition between these patterns in dorsomedial and lateral neocortex is marked with an arrow. **(b)** In sagittal sections of *Lhx2* cKO-E mice, anterior (A) neocortex exhibited aberrant three-layer cytoarchitecture of ePC and posterior (P) neocortex resembled six-layer cytoarchitecture observed dorsomedially in coronal sections. In *Lhx2* cKO-E mice, *Satb2* and *Ctip2* exhibited expression patterns appropriate for neocortex posteriorly and for piriform cortex anteriorly, coincident with cytoarchitecture change. The transition between these two patterns is marked with an arrow. *Satb2* expression persisted in ePC, albeit at reduced levels, but was not expressed in wild-type piriform cortex. The ePC was positioned dorsal to rhinal fissure (arrowhead). Scale bars represent 1.0 mm **(a)** and 1.5 mm **(b)**.

input from olfactory bulb to layers 1 and 3, as is seen in wild-type piriform cortex²³. However, in contrast with wild-type mice, the olfactory bulb projection in cKO-E mice continued beyond ePC and aberrantly projected into layer 1 throughout much of the neocortex (Fig. 5), consistent with lateral neocortex being re-fated into ePC and the gradual transitioning of ePC into neocortex.

Wild-type piriform cortex is absent in P7 *Lhx2* cKO-E mice

Although we found an Nrp2-positive, three-layer olfactory cortical structure ventral to ePC in P7 cKO-E, it did not express piriform cortex-specific markers and was identified as olfactory tubercle. This lack of an identifiable piriform cortex at its normal ventral position could be a result of either its failure to express piriform

Figure 5 The ePC in lateral neocortex of *Lhx2* cKO-E mice receives input from olfactory bulb similar to piriform cortex in wild-type mice. **(a–f)** Coronal sections of P7 wild-type **(a,b)**; *Lhx2^{loxP/−}* and *Lhx2* cKO-E **(d,e)**; *Lhx2^{loxP/−}; Emx1-cre* brains in which the axon tracer Dil (red) was placed in the olfactory bulb (arrowhead in **c** and **f**) to label its axonal projection through the lateral olfactory tract to layers 1 and 3 of piriform cortex. Sections were counterstained with DAPI (blue). In wild type, olfactory bulb axons formed the lateral olfactory tract (arrowhead) and projected to piriform cortex **(a)**. Higher magnification of the region near the arrowhead in **a** revealed the termination of olfactory bulb axons mainly in layers 1 and 3 **(b)**. In *Lhx2* cKO-E mice, the presumptive lateral olfactory tract (arrowhead) shifted dorsally and the axonal projection from olfactory bulb terminated in the ePC in lateral neocortex (its dorsal border is marked by an arrow, **d**). The olfactory bulb projection aberrantly extended through layer 1 of the neocortex, but was restricted to the ePC in layer 3. A higher magnification of the region near the arrowhead in **d** showing the terminations of olfactory bulb axons mainly in layers 1 and 3 in the ePC in *Lhx2* cKO-E mice, as in wild type, is shown in **e**. Scale bars represent 0.5 mm **(a,d)**, 0.2 mm **(b,e)** and 0.5 mm **(c,f)**.

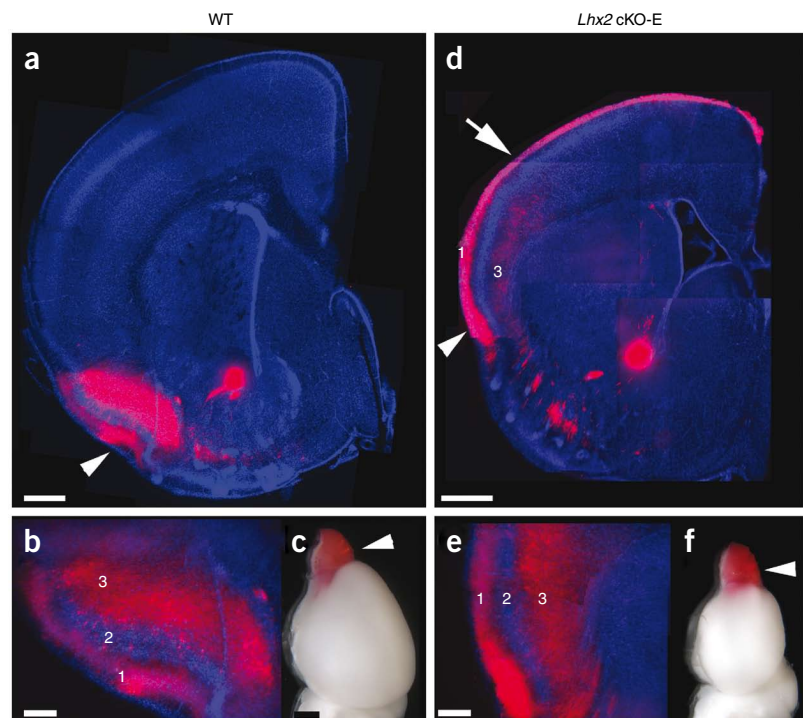
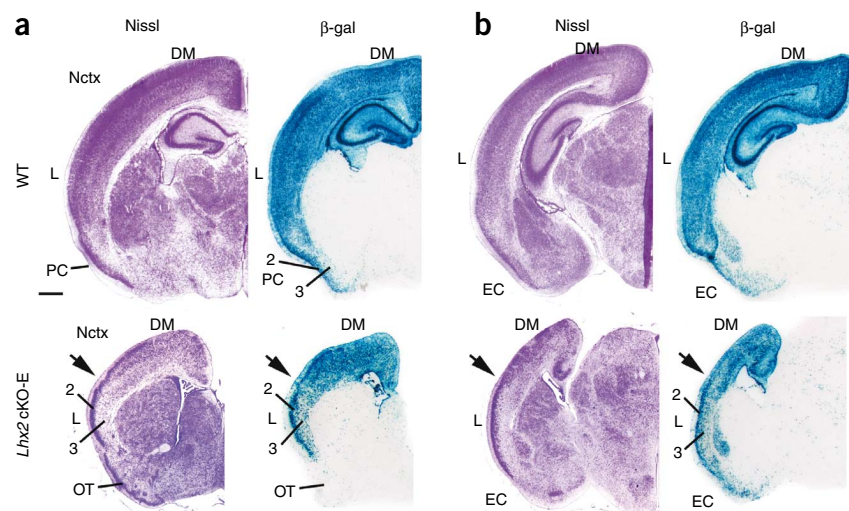


Figure 6 The ePC located in the lateral neocortex in *Lhx2* cKO-E mice is generated by an *Emx1* lineage, whereas wild-type piriform cortex is not evident. (a,b) Nissl and β -galactosidase (β -gal) staining on adjacent coronal sections of P7 wild-type (*Lhx2^{loxP/+}; Emx1-cre; R26R*) and *Lhx2* cKO-E (*Lhx2^{loxP/-}; Emx1-cre; R26R*) brains at two different levels (a, anterior; b, posterior). Blue cells are β -galactosidase labeled and are of the *Emx1* lineage; the density of the β -galactosidase-labeling patterns paralleled the neuronal density revealed by Nissl staining. In wild type, the entire six-layer neocortex (Nctx) was labeled by β -galactosidase. In three-layer piriform cortex, layer 2 was intensely labeled and layer 3 had scattered labeled cells. In *Lhx2* cKO-E mice, the neocortex was also well labeled by β -galactosidase. In dorsomedial neocortex, the six cortical layers were all labeled, and layer 2 was intensely labeled and layer 3 showed sparse labeling in the ePC in lateral neocortex, consistent with the density of neurons shown by Nissl staining and with β -galactosidase labeling in wild-type piriform cortex. The transitions between the six-layer and three-layer patterns in dorsomedial neocortex and lateral neocortex (that is, ePC), respectively, are marked with arrows. Scale bar represents 0.2 mm. EC, entorhinal cortex.



cortex-specific markers following deletion of *Lhx2* or of wild-type piriform cortex not being present. To distinguish between these possibilities, we carried out an *Emx1* lineage analysis by crossing the *Emx1-cre* line with the ROSA26 reporter line²⁴ on wild-type and cKO-E mutant backgrounds, permanently labeling all of the cells of the *Emx1* lineage with β -galactosidase.

In P7 wild-type mice, neocortex and piriform cortex were well labeled by β -galactosidase (Fig. 6). The density of β -galactosidase labeling paralleled the neuronal density revealed by Nissl staining, confirming that neocortex and piriform cortex were formed predominantly by neurons of the *Emx1* lineage. In contrast, few β -galactosidase-labeled cells were found in olfactory tubercle (Fig. 6), indicating that it was derived from lineages other than *Emx1*. In P7 cKO-E mice, dorsomedial neocortex was heavily labeled by β -galactosidase, as was ePC in the location normally occupied by lateral neocortex; in both, the density of labeled cells mirrored that observed in adjacent Nissl stained sections, as was seen in wild-type mice (Fig. 6a). At caudal positions, beyond the normal anterior-posterior extent of piriform cortex in wild-type mice, the β -galactosidase-labeled entorhinal cortex was ventral to lateral neocortex, whereas in cKO-E mice, the β -galactosidase-labeled entorhinal cortex was ventral to ePC positioned in lateral neocortex (Fig. 6b). At more rostral levels, where piriform cortex was found in wild-type mice, we did not find a β -galactosidase-labeled structure ventral to β -galactosidase-labeled ePC positioned in lateral neocortex; instead, this ventral position was occupied by β -galactosidase-negative olfactory tubercle. These findings confirm our observations that wild-type piriform cortex is not present at its normal ventral position in cKO-E at P7 and the only piriform cortex-like structure is ePC positioned in lateral neocortex.

ePC is not wild-type piriform cortex shifted dorsally

The most straightforward interpretation of our findings in cKO-E mice is that progenitors that generate lateral neocortex are re-fated as a result of *Lhx2* deletion to generate neurons of piriform cortex rather than neocortex. Alternatively, because of the reduced size of cortex in cKO-E mice, wild-type piriform cortex has shifted dorsally to an ectopic position normally occupied by lateral neocortex. The positioning of ePC relative to the rhinal fissure, a sulcus that is

constant across mammalian species and separates neocortex located dorsal to it from paleocortical piriform cortex located ventral to it²⁵, argues against this alternative. In wild-type mice, piriform cortex was positioned ventral to the rhinal fissure, whereas in cKO-E mice, ePC was positioned dorsal to the rhinal fissure, where lateral neocortex is found in wild-type mice (Fig. 4 and Supplementary Fig. 3). This finding is consistent with the idea that ePC is produced by progenitors that are a part of the pool of neocortical progenitors, albeit re-fated as a result of *Lhx2* deletion, that continues to generate neurons that form a continuous sheet of cells that are distinct from wild-type piriform cortex.

Although positioning of ePC relative to the rhinal fissure makes it virtually inconceivable that ePC is actually wild-type piriform cortex that has shifted dorsally, we nonetheless directly addressed whether ectopic positioning of piriform cortex dorsal to the rhinal fissure is the result of reduced cortical size. To test this hypothesis, we crossed *Lhx2^{loxP/loxP}* mice with a *Nestin-cre* line⁹ and analyzed telencephalic patterning in offspring (cKO-N mice; Fig. 3). At P7, cortices of cKO-E and cKO-N mice were similar in size, both being approximately half the size of the cortices of wild-type mice (Fig. 7a,b). In contrast with cKO-E mice, however, piriform cortex identified by expression of the paleocortical marker *Nrp2* and the piriform cortex-specific markers *Slc6a7* and *Liprin β 1* (Fig. 3) in cKO-N mice was positioned ventrally, similar to wild-type piriform cortex; in addition, lateral neocortex was also normally positioned and had a six-layer architecture (Figs. 3 and 7). These findings refute the possibility that the exaggerated dorsal position of ePC above the rhinal fissure in cKO-E is a secondary result of reduced cortical size.

ePC is substantially larger than wild-type piriform cortex

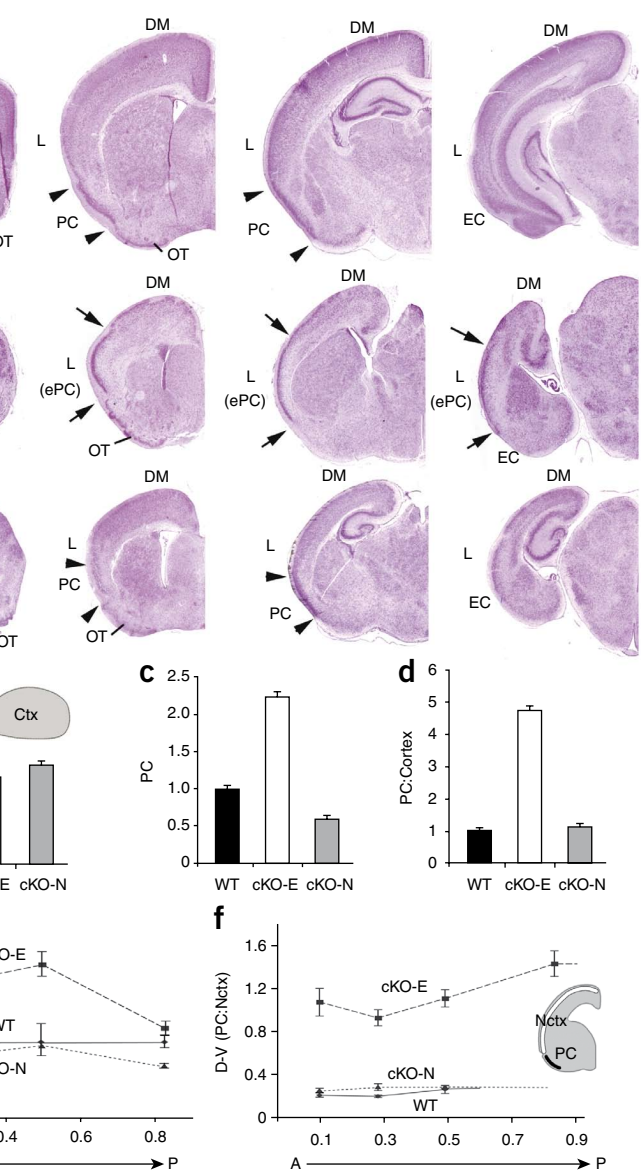
The position of ePC relative to that of wild-type piriform cortex and lateral cortex and the fact that it was significantly larger than piriform cortex in wild-type mice ($P < 0.001$) provides an additional argument that the ePC was generated, in large part if not entirely, by re-fated neocortical progenitors (Fig. 7). First, ePC in cKO-E mice was positioned dorsal to the rhinal fissure, at the location of lateral neocortex in wild-type mice, and ePC was found at the location of lateral neocortex along the entire anterior-posterior extent of neocortex, including well posterior to the normal extent of piriform cortex in

Figure 7 Size and extent of ePC in cKO-E mice and piriform cortex in wild-type and cKO-N mice. (a) Nissl staining of anterior (left) to posterior (right) coronal brain sections of P7 wild type, cKO-E and cKO-N. Piriform cortex (PC) in wild type and cKO-N (arrowheads) and ePC in cKO-E (arrows) are marked. EC, entorhinal cortex. (b) Surface area of cerebral cortex. cKO-E ($n = 4$, $P < 0.001$, unpaired Student's t test) and cKO-N areas ($n = 2$, $P < 0.001$) were smaller than wild type ($n = 8$). (c) Piriform cortex size. cKO-E ePC ($n = 4$) was larger ($P < 0.001$) and cKO-N piriform cortex ($n = 3$) was smaller ($P < 0.001$) than wild-type piriform cortex ($n = 6$). (d) Ratio of piriform cortex size to cortical size (PC:cortex). ePC:cortex in cKO-E ($n = 4$) was larger ($P < 0.001$) than PC:cortex in wild type ($n = 6$) and cKO-N ($n = 3$). (e) Dorsal-ventral length of piriform cortex at positions along the anterior-posterior extent of piriform cortex. cKO-N piriform cortex ($n = 3$) was smaller than wild-type piriform cortex ($n = 6$); cKO-E ePC ($n = 4$) was larger than both ($P < 0.001$). (f) Dorsal-ventral length of piriform cortex relative to neocortex (PC:Nctx) at positions along the cortical anterior-posterior axis. In wild-type and cKO-N mice, piriform cortex was limited to rostral 60% and 79% of cortical anterior-posterior axis; cKO-E ePC was found along entire extent. ePC:Nctx in cKO-E ($n = 4$) was greater than PC:Nctx in wild-type ($n = 6$) or cKO-N ($n = 3$) ($P < 0.001$), which are similar. cKO data normalized to the mean of the measured feature in wild type, which was set as 1, for b–f. Scale bar represents 0.5 mm. Error bars indicate \pm s.e.m.

wild-type mice, covering essentially 100% of the anterior-posterior cortical axis. In contrast, wild-type piriform cortex was limited to the rostral 60% of the anterior-posterior cortical axis in wild-type and 79% in cKO-N mice (Fig. 7a,f). Furthermore, ePC was significantly longer along the dorsal-ventral telencephalic axis than wild-type piriform cortex in either wild-type or cKO-N mice ($P < 0.001$; Fig. 7a,e,f). At each anterior-posterior position, ePC was proportionally larger than wild-type piriform cortex and accounted for between 50% and 60% of the dorsal-ventral cortical axis in cKO-E mice, whereas piriform cortex in both wild-type and cKO-N mice accounted for 25% or less (Fig. 7f). The absolute dorsal-ventral extent of ePC in cKO-E mice was also greater than wild-type piriform cortex, with ePC being up to 200% of the absolute dorsal-ventral extent of wild-type piriform cortex (Fig. 7a,e). Furthermore, ePC size relative to neocortex was more than 400% greater in cKO-E mice than piriform cortex size relative to neocortex in wild-type mice (Fig. 7d); even in absolute total area, ePC was over twice the size of wild-type piriform cortex (Fig. 7c).

These findings can only be explained by one of two mechanisms. The best fit is that ePC is generated by re-fated progenitors of the Emx1 lineage that would normally generate lateral neocortex. The only alternative requires that progenitors that normally generate piriform cortex, which are localized to dTel PSB²⁶, undergo a substantial increase in proliferation in cKO-E mice to generate the larger ePC, coupled with an aberrantly quiescent population of progenitors that would normally generate lateral neocortex. However, this

mechanism is infeasible, as we found no evidence for substantial changes in distribution and relative densities of active progenitors using BrdU pulse labeling during neurogenesis at E11.5, E13.5 and E15.5 (Supplementary Fig. 4).



mechanism is infeasible, as we found no evidence for substantial changes in distribution and relative densities of active progenitors using BrdU pulse labeling during neurogenesis at E11.5, E13.5 and E15.5 (Supplementary Fig. 4).

Wild-type piriform cortex is transiently present in cKO-E

To provide definitive evidence that progenitors of the Emx1 lineage that normally generate lateral neocortex are re-fated to generate an ePC in cKO-E mice, we carried out the Emx1 lineage analysis described above at embryonic and perinatal ages. For this, the *Emx1-cre* and ROSA26 reporter lines were crossed and the offspring were analyzed on wild-type and cKO-E backgrounds.

In E13.5 and E15.5 wild-type embryos, both neocortex and the piriform cortex positioned ventral to it were formed by a high density of neurons labeled with β -galactosidase, indicating that they were the progeny of progenitors of the Emx1 lineage (Fig. 8). In E13.5 cKO-E mice, the distribution, number and density of β -galactosidase-labeled neurons closely resembled those in E13.5 wild-type littermates; both neocortex and piriform cortex were readily identified at their normal positions (Fig. 8a). The wild-type piriform cortex remained evident

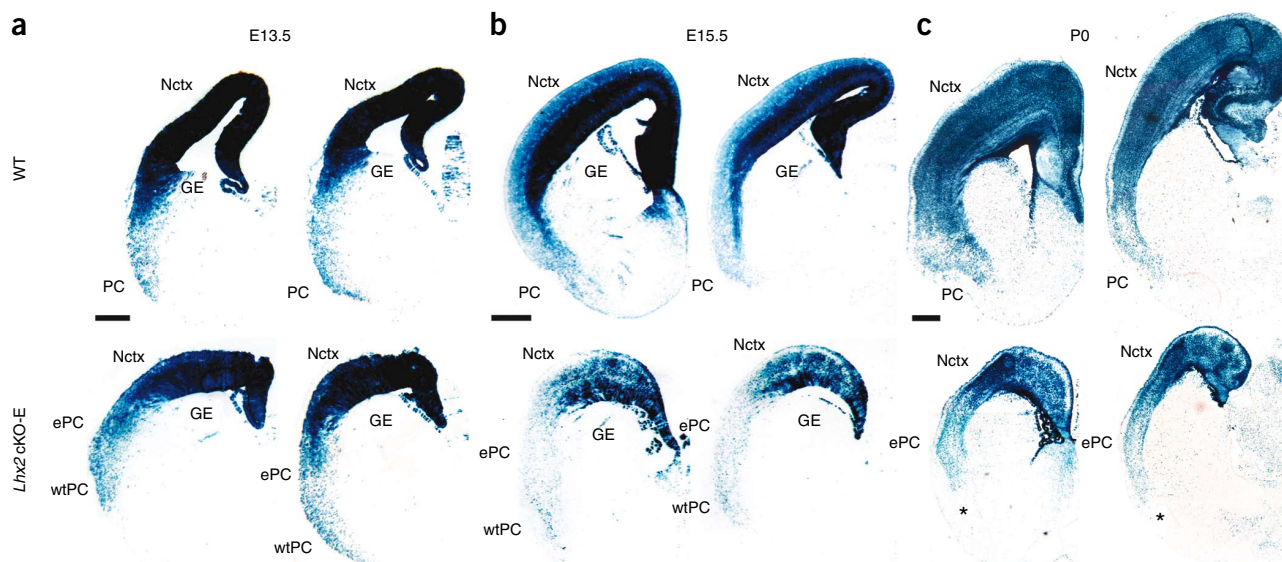


Figure 8 Wild-type piriform cortex is generated and forms at appropriate ventral position in *Lhx2* cKO-E mice but is subsequently eliminated. (a–c) β -galactosidase staining on coronal sections of E13.5 (a), E15.5 (b) and P0 (c) wild-type (*Lhx2^{loxP/+}; Emx1-cre; R26R*) and *Lhx2* cKO-E (*Lhx2^{loxP/-}; Emx1-cre; R26R*) brains at two different levels (left, anterior; right, posterior). Blue cells are labeled by β -galactosidase, indicating that the cells belong to the *Emx1* lineage that forms the cerebral cortex, including neocortex and piriform cortex. (a) At E13.5, in both wild-type and *Lhx2* cKO-E mice, the neocortex and piriform cortex, as well as other regions of cerebral cortex, had a high density of β -galactosidase-labeled neurons. In *Lhx2* cKO-E mice, both the ePC and the wild-type piriform cortex (wtPC) were evident. (b) At E15.5, in wild type, the distribution and density of β -galactosidase-labeled neurons was similar to E13.5. In *Lhx2* cKO-E, however, a reduction in the number and density of β -galactosidase-labeled neurons was evident in the wild-type piriform cortex, whereas the neocortex, especially the ventricular zone, remained strongly labeled by β -galactosidase. (c) At P0, the wild-type piriform cortex was no longer evident in the *Lhx2* cKO-E mice, but remained well labeled in wild type. The position where the wild-type piriform cortex would be positioned were it present in the *Lhx2* cKO-E mice is indicated by the asterisk; dorsal to this position, the ePC can be identified by the patterned distribution of β -galactosidase-labeled cells. Scale bars represent 0.2 mm (a) and 0.5 mm (b,c). GE, ganglionic eminence.

at E15.5 in cKO-E mice at its normal ventral position, but the density of β -galactosidase-labeled neurons was reduced compared with E15.5 wild-type littermates and cKO-E mice observed 2 d prior, at E13.5 (Fig. 8b). Consistent with our identification of this ventrally located piriform cortex in cKO-E mice as wild-type piriform cortex, it was positioned at the ventral-most location of the migrational scaffold between the dTel ventricular zone and the cortical wall formed by the *Fabp7* (BLBP)-positive processes of radial glia, the progenitors of the *Emx1* lineage. At this ventral-most position, a particularly dense bundle of the radial glial processes formed a palisade that connected the ventricular zone of the PSB to the telencephalic wall²⁷ in both cKO-E and wild-type mice and formed a migrational guide for wild-type piriform cortex neurons (Supplementary Fig. 5).

Elimination of β -galactosidase-labeled wild-type piriform cortex neurons continued over the next few days such that wild-type piriform cortex was no longer identifiable in cKO-E mice by P0 (Fig. 8c), as it was at P7 (Fig. 6). Because this method of lineage tracing permanently marked piriform cortex neurons observed at E13.5 in both wild-type and cKO-E mice, the only possible explanation for the early presence of a piriform cortex at its normal ventral position and later absence in cKO-E mice is that wild-type piriform cortex was generated and formed, but was subsequently eliminated. Crossing *Lhx2^{loxP/loxP}* mice with a *Nex-cre* mouse line that deletes *Lhx2* from postmitotic neurons immediately after their generation¹⁰ had no effect on viability of wild-type piriform cortex, indicating that its elimination in cKO-E mice is a result of a defect resulting from deletion of *Lhx2* from dTel progenitors that is inherited by piriform cortex neurons (Supplementary Fig. 6). These results, interpreted in the context of other findings, provide evidence that ePC observed at P7 in cKO-E mice at the position of

lateral neocortex is not wild-type piriform cortex that has aberrantly shifted dorsally to the rhinal fissure and instead must be generated by progenitors of the *Emx1* lineage that are normally fated to generate lateral neocortex, but that, following deletion of *Lhx2* by *Emx1-cre*, are re-fated to generate piriform cortex.

Critical period for *Lhx2* regulation of regional fate

Unlike cKO-E mice, cKO-N mice did not form an ePC in place of lateral neocortex and instead had a piriform cortex that resembled wild-type piriform cortex in size and position. Because *Emx1* and *Nestin* drivers both produce Cre expression in all of the progenitors of the *Emx1* lineage in the dTel ventricular zone, this difference in phenotype must be a result of differences in the timing of Cre expression and recombination. Indeed, recombination produced by *Emx1-cre* mice was not detectable at E9.5, but was robust at E10.5, whereas recombination produced by *Nestin-cre* mice was not detectable at E10.5, but was robust at E11.5 (Supplementary Fig. 7). Thus, the *Nestin-cre* line produced recombination 1 d later than the *Emx1-cre* line. These findings define a critical period for *Lhx2* regulation of the fate decision to generate lateral neocortical neurons or piriform cortex neurons, which occurs between E10.5 and E11.5.

Defining this critical period leads to predictions of a transition zone between the neocortex and ePC in cKO-E mice on the basis of the rostro-lateral-to-caudomedial temporal gradient of corticogenesis across the neocortical axes²⁸. This transition zone is characterized by a mix of neurons with neocortical or piriform cortex properties in a radial traverse at the medial edge of ePC at a location along the temporal neurogenic gradient, where timing of Cre-mediated deletion of *Lhx2* from progenitors straddles the critical period. To address this issue, we analyzed the

expression of *Satb2* relative to *Ctip2*, which marked layer 5 of neocortex, and also layer 2 of piriform cortex (Fig. 4). The predicted transition zone was indeed observed (Supplementary Fig. 8), providing further evidence of a critical period for *Lhx2* regulation of regional fate.

To begin assessing the genetic hierarchy that accounts for re-fating of cortical progenitors following early *Lhx2* deletion, we analyzed the expression of *Emx1*, *Pax6* and *Neurog2* (*Ngn2*), transcription factors involved in cell specification and patterning in forebrain, in the dTel ventricular zone^{29,30}. Because progenitors of the *Emx1* lineage undergo a fate change in cKO-E mice, but not in cKO-N mice, transcription factors that are differentially expressed in cKO-E mice are potentially involved with this fate decision. However, each transcription factor that we analyzed was similarly downregulated in both cKO-E and cKO-N mice (Supplementary Fig. 9), indicating that they are unlikely to have an instructive role in mediating the neocortical versus piriform cortex fate decision.

DISCUSSION

We found that *Lhx2* regulates a genetic mechanism that is intrinsic to dTel progenitors of the *Emx1* lineage and that determines their regional fate in generating cerebral cortex. Following *Lhx2* deletion at E10.5 by *Emx1-cre*, the cortical hemisphere of cKO-E offspring was reduced to half of the size of that seen in wild-type, and the neocortex had two position-dependent and continuous architectures; dorso-medially, the neocortex had a six-layer architecture that resembled that of wild-type neocortex, albeit with localized laminar defects, and that transitioned laterally into a three-layer structure that phenocopied the architecture, marker expression and connectivity of piriform cortex. This ePC was considerably larger than wild-type piriform cortex and developed at the location of lateral neocortex along the entire anterior-posterior extent of the cortical hemisphere, extending well beyond the anterior-posterior extent of wild-type piriform cortex. Lineage tracing showed that wild-type piriform cortex itself was also generated and formed at its normal position ventral to neocortex, but was subsequently eliminated. We provide evidence that ePC was generated by dTel progenitors of the *Emx1* lineage that are normally fated to generate lateral neocortex, but were re-fated following early deletion of *Lhx2* to generate piriform cortex (Supplementary Results and Supplementary Fig. 10).

Use of the *Nestin-cre* transgene resulted in the deletion of *Lhx2* at E11.5, 1 d after *Lhx2*'s deletion by *Emx1-cre*, and cKO-N offspring had a reduced cortical size, similar to that in cKO-E mice produced by *Emx1-cre*. However, cKO-N mice did not develop an ePC and instead had a uniform neocortex with six-layer architecture that resembled wild-type neocortex and a piriform cortex of normal size and viability at the appropriate wild-type location ventral to lateral neocortex. These distinct phenotypes reveal a critical period for *Lhx2* regulation of the fate decision by dTel progenitors of the *Emx1* lineage to generate neocortex or paleocortical piriform cortex and suggest that closing of the critical period, characterized by a restriction in regional fate of these progenitors, occurs between E10.5 and E11.5.

Mechanisms for determining regional fates in *Emx1* lineage

Cerebral cortex is a hierarchically patterned structure divided anatomically and functionally into specialized regions, which in turn are divided into anatomically and functionally distinct areas that serve unique modalities¹. Neocortical areas are specified through the action of transcription factors expressed in graded patterns along the anterior-posterior and dorsal-ventral cortical axes²⁹. For example, area patterning of neocortex is regulated in part by the homeodomain

transcription factor *Emx2*, with the expression level of *Emx2* in particular being a critical determinant of area identity of a progenitor in the neocortical ventricular zone³¹.

The mechanism for determining the regional fate of cerebral cortex by *Lhx2* may be similar to that used to determine the areal fate of neocortex by *Emx2*, as both are expressed in a high caudomedial to low rostralateral gradient and act on dTel progenitors of the *Emx1* lineage. Although we have not shown that the graded feature of *Lhx2* expression is an important determinant for regulating regional fate among dTel progenitors of the *Emx1* lineage, the graded position-dependent level of *Lhx2* expression in wild-type mice is probably the feature that distinguishes the progenitors of lateral neocortex from those that generate piriform cortex. *Lhx2* could act by repressing piriform cortex fate or inducing piriform cortex fate over specific ranges of expression. Our findings suggest that either piriform cortex is the default regional fate for lateral neocortical progenitors following deletion of *Lhx2* on E10.5 or that a progenitor's regional fate is determined by its 'exposure' to *Lhx2*, which is the product of exposure time and expression level, with the exposure experienced by lateral neocortical progenitors following *Lhx2* deletion on E10.5 (*Emx1-cre*) leading to a piriform cortex fate and *Lhx2* deletion on E11.5 (*Nestin-cre*) leading to a neocortical fate.

Implications for critical period and cortical evolution

The difference in the timing of *Lhx2* deletion between cKO-E and cKO-N and their different phenotypes reveal a critical period for *Lhx2* regulation of the fate decision to generate neocortical or piriform cortex neurons and suggest that the closing of the critical period occurs between E10.5 and E11.5. The timing of this regional fate restriction is coincident with the onset of cortical neurogenesis³², which itself is determined by substantial differentiation of cortical progenitors, specifically transition of neuroepithelial cells into neuronogenic radial glia³³. The timing of the critical period for *Lhx2* function in regulating regional fate indicates that determination of regional fate is made by neuroepithelial cells and is plastic during their stage of symmetric divisions, but becomes restricted with their transition into radial glia and the asymmetric division stage. A recent study of regulation of this transition period of progenitor differentiation found that the area fates of dTel progenitors that generate neocortex are determined in neuroepithelial cells and become fixed before their differentiation into radial glia³⁴. Our findings suggest that the critical period for regional fate of cerebral cortex also correlates with timing of the transition from neuroepithelial cell to radial glia, suggesting that the critical periods for regional fate and areal fate are similar.

Progenitors that give rise to dorsomedial and lateral neocortex exhibit a substantial difference in their retention of neocortical properties versus re-fating into olfactory cortical progenitors following early deletion of *Lhx2* by *Emx1-cre*. This difference may be a result of the two neocortical domains having different critical periods, with the critical period for the dorsomedial neocortex closing earlier than that for the lateral neocortex, or may be a result of a substantial genetic distinction between progenitors of the *Emx1* lineage that give rise to dorsomedial versus lateral neocortex. Determining whether progenitors of dorsomedial neocortex have an earlier critical period will distinguish between these two alternatives. However, we currently do not have a Cre mouse line that would delete *Lhx2* at an age earlier than *Emx1-cre* and still result in a viable mouse with an intact cerebral cortex.

Our findings support classic models of cortical evolution that have fallen out of favor. For example, a dual-origin model postulates that

paleocortex contributes to lateral neocortex and archicortex to dorso-medial neocortex, which is supported by our finding in cKO-E mice that lateral neocortex re-fated into paleocortical piriform cortex, whereas dorsomedial neocortex retained a neocortical-like fate. Our findings also support a model in which both piriform cortex and neocortex have evolved from ventrolateral telencephalon^{1,35–37}. Specifically, we found that the dTel progenitors of the Emx1 lineage that generate piriform cortex and neocortex were genetically almost identical, at least as neuroepithelial cells before their fate restriction, with only the expression level of Lhx2 functionally distinguishing them. Thus, Lhx2 specification of regional-fate of cerebral cortex serves a critical role during development and likely also during evolution.

METHODS

Methods and any associated references are available in the online version of the paper at <http://www.nature.com/natureneuroscience/>.

Note: Supplementary information is available on the Nature Neuroscience website.

ACKNOWLEDGMENTS

We thank B. Higgins and H. Gutierrez for technical assistance, Y. Nakagawa for help with screening for Lhx2 genomic DNA, K. Jones for *Emx1-cre* mice, K.-A. Nave for *Nex-cre* mice, and P.M. Soriano for *ROSA26-LacZ* reporter mice. This work was supported by grants from the US National Institutes of Health to D.D.M.O.

AUTHOR CONTRIBUTIONS

S.-J.C. designed and generated the *loxP*-flanked allele of Lhx2, was a principal contributor to analysis of the *Lhx2* conditional knockouts, prepared figures and assisted with the writing of the paper. C.G.P.-G. was a principal contributor to the analysis of the *Lhx2* conditional knockouts, prepared figures and assisted with the writing of the paper. T.T.K. contributed to the analysis of the *Lhx2* conditional knockouts and help to prepare the figures. D.D.M.O. conceived the study, designed and contributed to the analysis of the *Lhx2* conditional knockouts, prepared figures and wrote the paper.

Published online at <http://www.nature.com/natureneuroscience/>.

Reprints and permissions information is available online at <http://www.nature.com/reprintsandpermissions/>.

- Sanides, F. Comparative architectonics of the neocortex of mammals and their evolutionary interpretation. *Ann. NY Acad. Sci.* **167**, 405–423 (1969).
- Bishop, K.M., Rubenstein, J.L.R. & O'Leary, D.D.M. Distinct actions of *Emx1*, *Emx2* and *Pax6* in regulating the specification of areas in the developing neocortex. *J. Neurosci.* **22**, 7627–7638 (2002).
- Porter, F.D. *et al.* Lhx2, a LIM homeobox gene, is required for eye, forebrain and definitive erythrocyte development. *Development* **124**, 2935–2944 (1997).
- Bulchand, S., Grove, E.A., Porter, F.D. & Tole, S. LIM-homeodomain gene Lhx2 regulates the formation of the cortical hem. *Mech. Dev.* **100**, 165–175 (2001).
- Vyas, A., Saha, B., Lai, E. & Tole, S. Paleocortex is specified in mice in which dorsal telencephalic patterning is severely disrupted. *J. Comp. Neurol.* **466**, 545–553 (2003).
- Monuki, E.S., Porter, F.D. & Walsh, C.A. Patterning of the dorsal telencephalon and cerebral cortex by a roof plate–Lhx2 pathway. *Neuron* **32**, 591–604 (2001).
- Mangale, V.S. *et al.* Lhx2 selector activity specifies cortical identity and suppresses hippocampal organizer fate. *Science* **319**, 304–309 (2008).
- Gorski, J.A. *et al.* Cortical excitatory neurons and glia, but not GABAergic neurons, are produced in the *Emx1*-expressing lineage. *J. Neurosci.* **22**, 6309–6314 (2002).
- Graus-Porta, D. *et al.* Beta1-class integrins regulate the development of laminae and folia in the cerebral and cerebellar cortex. *Neuron* **31**, 367–379 (2001).
- Goebbels, S. *et al.* Genetic targeting of principal neurons in neocortex and hippocampus of NEX-Cre mice. *Genesis* **44**, 611–621 (2006).
- Britanova, O. *et al.* *Satb2* is a postmitotic determinant for upper-layer neuron specification in the neocortex. *Neuron* **57**, 378–392 (2008).
- Chen, H., Chedotal, A., He, Z., Goodman, C.S. & Tessier-Lavigne, M. Neuropilin-2, a novel member of the neuropilin family, is a high affinity receptor for the semaphorins Sema E and Sema IV, but not Sema III. *Neuron* **19**, 547–559 (1997).
- Grove, E.A., Tole, S., Limon, J., Yip, L. & Ragsdale, C.W. The hem of the embryonic cerebral cortex is defined by the expression of multiple Wnt genes and is compromised in *Gli3*-deficient mice. *Development* **125**, 2315–2325 (1998).
- Assimacopoulos, S., Grove, E.A. & Ragsdale, C.W. Identification of a *Pax6*-dependent epidermal growth factor family signaling source at the lateral edge of the embryonic cerebral cortex. *J. Neurosci.* **23**, 6399–6403 (2003).
- Anderson, S., Mione, M., Yun, K. & Rubenstein, J.L.R. Differential origins of neocortical projection and local circuit neurons: role of *Dlx* genes in neocortical interneuronogenesis. *Cereb. Cortex* **9**, 646–654 (1999).
- Casarosa, S., Fode, C. & Guillemot, F. *Mash1* regulates neurogenesis in the ventral telencephalon. *Development* **126**, 525–534 (1999).
- Colombo, E., Galli, R., Cossu, G., Gecz, J. & Broccoli, V. Mouse orthologue of *ARX*, a gene mutated in several X-linked forms of mental retardation and epilepsy, is a marker of adult neural stem cells and forebrain GABAergic neurons. *Dev. Dyn.* **231**, 631–639 (2004).
- Yun, K., Garel, S., Fischman, S. & Rubenstein, J.L.R. Patterning of the lateral ganglionic eminence by the *Gsh1* and *Gsh2* homeobox genes regulates striatal and olfactory bulb histogenesis and the growth of axons through the basal ganglia. *J. Comp. Neurol.* **461**, 151–165 (2003).
- Matsuoka, H., Obama, H., Kelly, M.L., Matsui, T. & Nakamoto, M. Biphasic functions of the kinase-defective *Ephb6* receptor in cell adhesion and migration. *J. Biol. Chem.* **280**, 29355–29363 (2005).
- Höglund, P.J., Adzic, D., Scicluna, S.J., Lindblom, J. & Fredriksson, R. The repertoire of solute carriers of family 6: identification of new human and rodent genes. *Biochem. Biophys. Res. Commun.* **336**, 175–189 (2005).
- Kriajevska, M. *et al.* *Liprin beta 1*, a member of the family of LAR transmembrane tyrosine phosphatase-interacting proteins, is a new target for the metastasis-associated protein S100A4 (Mts1). *J. Biol. Chem.* **277**, 5229–5235 (2002).
- Arlotta, P. *et al.* Neuronal subtype-specific genes that control corticospinal motor neuron development *in vivo*. *Neuron* **45**, 207–221 (2005).
- Shipley, M.T. & Adamek, G.D. The connections of the mouse olfactory bulb: a study using orthograde and retrograde transport of wheat germ agglutinin conjugated to horseradish peroxidase. *Brain Res. Bull.* **12**, 669–688 (1984).
- Soriano, P. Generalized lacZ expression with the *ROSA26-cre* reporter strain. *Nat. Genet.* **21**, 70–71 (1999).
- Ariens-Kappers, C.U., Huber, G.C. & Crosby, E.C. *The Comparative Anatomy of the Nervous System of Vertebrates Including Man* (ed. Co, M.) (Macmillan, New York, 1936).
- Carney, R.S. *et al.* Cell migration along the lateral cortical stream to the developing basal telencephalic limbic system. *J. Neurosci.* **26**, 11562–11574 (2006).
- Hirata, T. *et al.* Mosaic development of the olfactory cortex with *Pax6*-dependent and -independent components. *Brain Res. Dev. Brain Res.* **136**, 17–26 (2002).
- Bayer, S.A. & Altman, J. *Neocortical Development* (Raven Press, New York, 1991).
- O'Leary, D.D.M., Chou, S.J. & Sahara, S. Area patterning of the mammalian cortex. *Neuron* **56**, 252–269 (2007).
- Schuermans, C. *et al.* Sequential phases of cortical specification involve Neurogenin-dependent and -independent pathways. *EMBO J.* **23**, 2892–2902 (2004).
- Hamasaki, T., Leingartner, A., Ringstedt, T. & O'Leary, D.D.M. *EMX2* regulates sizes and positioning of the primary sensory and motor areas in neocortex by direct specification of cortical progenitors. *Neuron* **43**, 359–372 (2004).
- Caviness, V.S. Jr. Neocortical histogenesis in normal and reeler mice: a developmental study based upon [³H]thymidine autoradiography. *Brain Res.* **256**, 293–302 (1982).
- Götz, M. & Huttner, W.B. The cell biology of neurogenesis. *Nat. Rev. Mol. Cell Biol.* **6**, 777–788 (2005).
- Sahara, S. & O'Leary, D.D.M. *Fgf10* regulates transition period of cortical stem cell differentiation to radial glia controlling generation of neurons and basal progenitors. *Neuron* **63**, 48–62 (2009).
- Abbie, A.A. Cortical lamination in a polyploid marsupial, *Perameles natusa*. *J. Comp. Neurol.* **76**, 509–536 (1942).
- Ulinski, P.S. *Dorsal Ventricular Ridge: A Treatise on Forebrain Organization in Reptiles and Birds* (Wiley, New York, 1983).
- Abowitz, F., Montiel, J., Morales, D. & Concha, M. Evolutionary divergence of the reptilian and the mammalian brains: considerations on connectivity and development. *Brain Res. Brain Res. Rev.* **39**, 141–153 (2002).

ONLINE METHODS

Gene targeting and generation and use of mice. The *Lhx2* gene targeting was carried out using homologous recombination in embryonic stem cells. A replacement targeting vector was designed to delete the first three exons of the *Lhx2* gene, including the transcription start site, and replace them with a neomycin-resistance gene (*PGK-neo*) flanked by two *FRT* sites. We used diphtheria toxin under the control of the phosphoglycerate kinase promoter (*Pgk1*) to select against random insertion events. Targeted embryonic stem cell clones were screened by Southern blot with probes A and B (**Fig. 1**) and by PCR (for the neo cassette: P3, 5'-ATG CCT GCT TGC CGA ATA TC-3'; P5, 5'-CCC ATA AAG AGA TGT ACA CC-3'; for the second *loxP* site: P7, 5'-CTT TAA CCA TGC CGA CGT GG-3'; P8, 5'-GAG AGG CAA ACC AAA GGC AAC-3') and were identified as *Lhx2^{loxP-neo/+}* clones. These clones were subsequently injected into C57BL/6J blastocysts and the resulting chimeras were then mated to C57BL/6J females to obtain germ-line transmission. Heterozygous mice (*Lhx2^{loxP-neo/+}*) were mated with *FLPe* mice³⁸ to remove the neo cassette. *Lhx2^{loxP/loxP}* mice were generated by crossing heterozygous mice and genotyping was performed by PCR using the P7 and P8 primers. *Lhx2^{loxP/loxP}* mice were mated to *Emx1-IRES-cre* mice⁸, generously provided by K. Jones (U. of Colorado, Boulder), *Nestin-cre* transgenic mice⁹ (obtained from The Jackson Laboratory) and *Nex-cre* mice¹⁰, generously provided by K.-A. Nave (Max Planck Institute of Experimental Medicine). Double heterozygous *Lhx2^{loxP/+}; Emx1-cre*, *Lhx2^{loxP/+}; Nestin-cre* and *Lhx2^{loxP/+}; Nex-cre* mice were viable and fertile. For the staging of embryos, midday of the day of the vaginal plug was considered as E0.5 and the day of birth was termed P0. All of the experiments were conducted in accordance with US National Institutes of Health guidelines and were approved by the Institutional Animal Use and Care Committee of the Salk Institute.

In situ hybridization. Antisense RNA probes for *Arx*, *Bmp7*, *Dlx2*, *Dlx5*, *Emx1*, *EphB6*, *Er81*, *Gsh2*, *Liprinβ1*, *Lhx2*, *Mash1*, *Ngn2*, *Nrp2*, *Pax6*, *Satb2*, *Sfrp2*, *Slc6a7*

and *Wnt3a* were labeled using a DIG-RNA labeling kit (Roche). *In situ* hybridization on 16–20- μ m cryostat sections and whole-mount *in situ* hybridization were performed as previously described³⁹.

Immunostaining and axonal tracing. Mice were killed by perfusion with cold 4% buffered paraformaldehyde (wt/vol) or Bouin fixative. For Nissl staining, 10–20- μ m-thick sections were stained with 0.5% cresyl violet (wt/vol) and then dehydrated through graded alcohols. We used rabbit antibody to *Satb2* (kindly provided by V. Tarabykin, Max Planck Institute of Experimental Medicine), mouse antibody to *Satb2* (Abcam), rabbit antibody to BLBP (Abcam), rabbit antibody to Bc11b (Ctip2, Novus Biologicals) and rat antibody to BrdU (Accurate Chemical & Scientific). For immunostaining, 10–20- μ m-thick sections (cryostat and paraffin) were developed following the standard DAB (di-amino-benzidine) colorimetric reaction (Vectastain, Vector). For immunofluorescence, we used a FITC-conjugated goat antibody to rabbit and a Cy3-conjugated donkey antibody to rabbit (Jackson). DiI (1,1'-dioctadecyl 3,3,3',3'-tetramethylindocarbocyanine perchlorate; Molecular Probes) tracing of olfactory bulb projections was done as previously described³⁹. Crystals of the fluorescent carbocyanide dyes were inserted in the olfactory bulbs and brains were incubated for 3–12 weeks in 4% paraformaldehyde. The brains were embedded in 5% low-melting agarose (wt/vol), cut into 100- μ m-thick coronal sections on a vibratome, counterstained with DAPI (4'-6-diamidino-2-phenylindole), mounted in 0.1 M phosphate buffer and photographed under fluorescent light. Each tracing experiment was repeated at least three times and the results were reproducible.

38. Rodríguez, C.I. *et al.* High-efficiency deleter mice show that *FLPe* is an alternative to *cre-loxP*. *Nat. Genet.* **25**, 139–140 (2000).

39. Armentano, M. *et al.* COUP-TFI regulates the balance of cortical patterning between frontal/motor and sensory areas. *Nat. Neurosci.* **10**, 1277–1286 (2007).